JOURNAL OF CATALYSIS **83**, 267–285 (1983)

Oxidation of Methane over Supported Precious Metal Catalysts

C. F. CULLIS AND B. M. WILLATT

Department of Chemistry, The City University, London, EC1V OHB; and J. & S. Sieger Limited, Poole, Dorset, England

Received November 19, 1982; revised March 22, 1983

Studies of the kinetics of methane oxidation over palladium and platinum catalysts supported on a number of metal oxides were made using a pulse-flow microreactor technique. The reaction was investigated at temperatures in the range 500–800 K using reactant mixtures with $CH_4:O_2$ ratios varying from 1 : 10 to 10 : 1. The supports themselves, with the exception of tin(IV) oxide, did not appreciably catalyze the oxidation reaction. Nevertheless, the activity of both palladium and platinum catalysts was enhanced by the use of metal oxides of large surface area, such as γ-aluminum(III) oxide. The support also influenced the ability of palladium to adsorb oxygen and there was a correlation between the adsorption capacity of the supported precious metal and its catalytic activity for methane oxidation. The presence of adsorbed oxygen was confirmed using X-ray photoelectron spectroscopy but oxygen adsorbed at high temperatures proved detrimental towards methane oxidation. Prolonged exposure of the precious metals to oxygen at high temperatures caused structural changes in palladium, although this did not occur with platinum. The different catalytic behaviour of palladium and platinum was attributed to the differing abilities of these precious metals to adsorb oxygen prior to reaction. Measurement by transmission electron microscopy of the diameters of palladium particles dispersed on a γ-aluminum(III) oxide support showed that the catalytic activity for methane oxidation was independent of particle size.

INTRODUCTION

A number of studies have been made of the oxidation of methane over supported palladium and platinum catalysts (Table 1), but relatively few of them have been carried out under conditions sufficiently similar to enable the catalytic behavior of the two precious metals to be compared directly with one another. However, Anderson *et al.* (*1*) compared the catalytic activity of supported palladium with that of platinum and some other precious metals, and Firth and Holland (*5*) studied methane oxidation over microcalorimetric beads coated with palladium, platinum, rhodium, and iridium.

A particular advantage of using precious metal catalysts in supported form is that the support disperses the metal over a greater surface area and reduces thermal degradation. In studies of the oxidation of methane over supported palladium catalysts using a microcalorimetric bead reactor, the nature of the support had little influence on the catalytic activity during a given experiment but nevertheless affected the long-term stability of the catalyst (*6*). The effects were attributed to the different tendency of the supports to retain water, which decreases the catalytic activity as a result of the conversion of palladium(II) oxide to the corresponding hydroxide (*6, 9*).

The present work was designed to elucidate, by means of a pulse-flow technique, the mechanism of the oxidation of methane over supported palladium and platinum catalysts and to uncover the role of the support in these reactions. In particular, studies were made of the adsorption of oxygen on the precious metal catalysts and of the part played by adsorbed oxygen in the oxidation of methane. Attempts were also made to assess the importance, in the overall reaction mechanism, of the particle size of the precious metal and of interactions between the metal and the support.

0021-9517/83 $3.00

TABLE 1

Previous Studies of the Oxidation of Methane over Supported Palladium and Platinum Catalysts

Supported catalyst	Experimental method	Reactant mixture	Temperature range (K)	Order in		Activation energy (kJ mol^{-1})[a]	Reference
				methane	oxygen		
Pd on Al_2O_3	Continuous flow reactor	CH_4 in O_2	473–673	—	—	88–92	Anderson *et al.* (*1*)
Pd on Al_2O_3	Pulse flow reactor	6–30 vol% CH_4 in O_2	573–613	—	—	70–100	Schwab and Watson (*2*)
Pd on Al_2O_3	Continuous flow reactor	CH_4 in O_2	593–653	1.0	0	—	Mezaki and Watson (*3*)
Pd on 13X molecular sieve	Microcalorimetric bead	CH_4 in $O_2 + N_2$	573–673	1.0	0	88	Firth and Holland (*4*)
Pd on Al_2O_3	Microcalorimetric bead	0.5–2 vol% CH_4 in O_2	623–773	—	0	140(50)	Firth and Holland (*5*)
Pd on $ThO_2 + Al_2O_3$	Microcalorimetric bead	0.5–5 vol% CH_4 in O_2	673–873	0.8	0	42–59	Cullis *et al.* (*6*)
Pd + Pt on Al_2O_3	Continuous flow reactor	3 vol% CH_4 in O_2	523–793	—	—	63(13)	Zozulya (*7*)
Pt on porous Al_2O_3	Continuous flow reactor	27 vol% CH_4 in $O_2 + N_2$	773–853	1.0	0.8	187(86)	Trimm and Lam (*8*)
Pt on nonporous Al_2O_3	Continuous flow reactor	27 vol% CH_4 in $O_2 + N_2$	773–853	1.0	1.0	167(75)	Trimm and Lam (*8*)

[a] Values in brackets refer to measurements made at temperatures above the transition point.

EXPERIMENTAL

Materials

Precious metal compounds. Palladium(II) oxide, platinum(IV) oxide (Adams catalyst), and tetraammine palladium(II) chloride and tetraammine platinum(II) chloride (both "specpure") were supplied by Johnson Matthey Limited. Palladium(II) nitrate ("laboratory reagent" grade) was obtained from BDH Limited.

Catalyst supports. γ-Aluminum(III) oxide (Brockmann grade II "for chromatographic purposes") was supplied by BDH Limited and was shown by X-ray diffraction to contain small amounts of κ- and ε-Al_2O_3, together with traces of α-, θ-, and χ-Al_2O_3. α-Aluminum(III) oxide ("AnalaR") was also obtained from BDH Limited. Silicon(IV) oxide ("silica gel for carbon monoxide determination," 60–120 mesh) was supplied by Hopkin and Williams Limited, as was titanium(IV) oxide ("pigment grade"), which consisted mainly of anatase but contained 11 wt% of rutile. A sample of pure rutile was supplied by Tioxide Limited. Thorium(IV) oxide was prepared by heating AnalaR thorium(IV) nitrate hexahydrate (BDH Limited) at 783 K for 30 min and then at 1523 K for 6 h. Tin(IV) oxide ("specpure") was obtained from Johnson Matthey Limited.

Preparation of supported catalysts. Precious metal catalysts, supported on powdered refractory metal oxides, were prepared with precious metal loadings ranging from 1 to 40 wt%. In most cases an aqueous solution of the precious metal compound was refluxed with the required weight of support and the water was then removed by boiling. With palladium(II) oxide catalysts only, the precious metal oxide and the support were mixed as a slurry in methanol and the alcohol was evaporated.

The resulting solids were dried at 400 K for several hours, crushed and sieved, the 100–200 mesh (75–150 μm) fraction being retained. They were then heated to 775 K in a current of helium or hydrogen for at least 15 h, when the precious metal salts were converted to the corresponding metals or their oxides. The use of lower conditioning temperatures (<700 K) produced catalysts which did not give reproducible results, whereas the use of higher temperatures caused severe agglomeration of the metal particles, particularly in the case of palladium.

Gases. These were all supplied by Air Products Limited. Methane (quoted minimum purity 99.5%) and oxygen (quoted minimum purity 99.6%) were condensed at 78 K and then distilled, the middle fractions being collected and used. Helium ("ultrapure" grade) had a certified minimum purity of 99.995% and was guaranteed to contain less than 1 ppm of oxygen and less than 10 ppm of nitrogen; it was further purified by passage through a Matheson gas purifier containing 13X molecular sieve. Hydrogen (quoted minimum purity 99.99%) was passed through traps at 78 K before use. Nitrogen (quoted minimum purity 99.999%) was used as supplied for surface area measurements.

Apparatus and Procedure

A pulse-flow microreactor was placed in the carrier-gas line of a gas chromatograph. Reactants were introduced into the gas stream upstream of the reactor and the products leaving it were swept into the gas chromatograph for analysis (Fig. 1a).

The microreactor, which was similar to that used by Cullis *et al.* (*10*) and which is shown in more detail in Fig. 1b, was designed so that a small catalyst bed, uniformly heated throughout its length, was exposed to a rectangular pulse of the reactant gases, the composition of which was changed only as a result of its reaction over the catalyst. The inner (2 mm i.d.) and outer (5 mm i.d.) tubes of the reactor were made of silica and held in place by a stainless steel head with Viton rubber O-ring seals. The annular gap between these tubes was less than 1 mm. The catalyst bed was 15 mm long and 2 mm in diameter and was

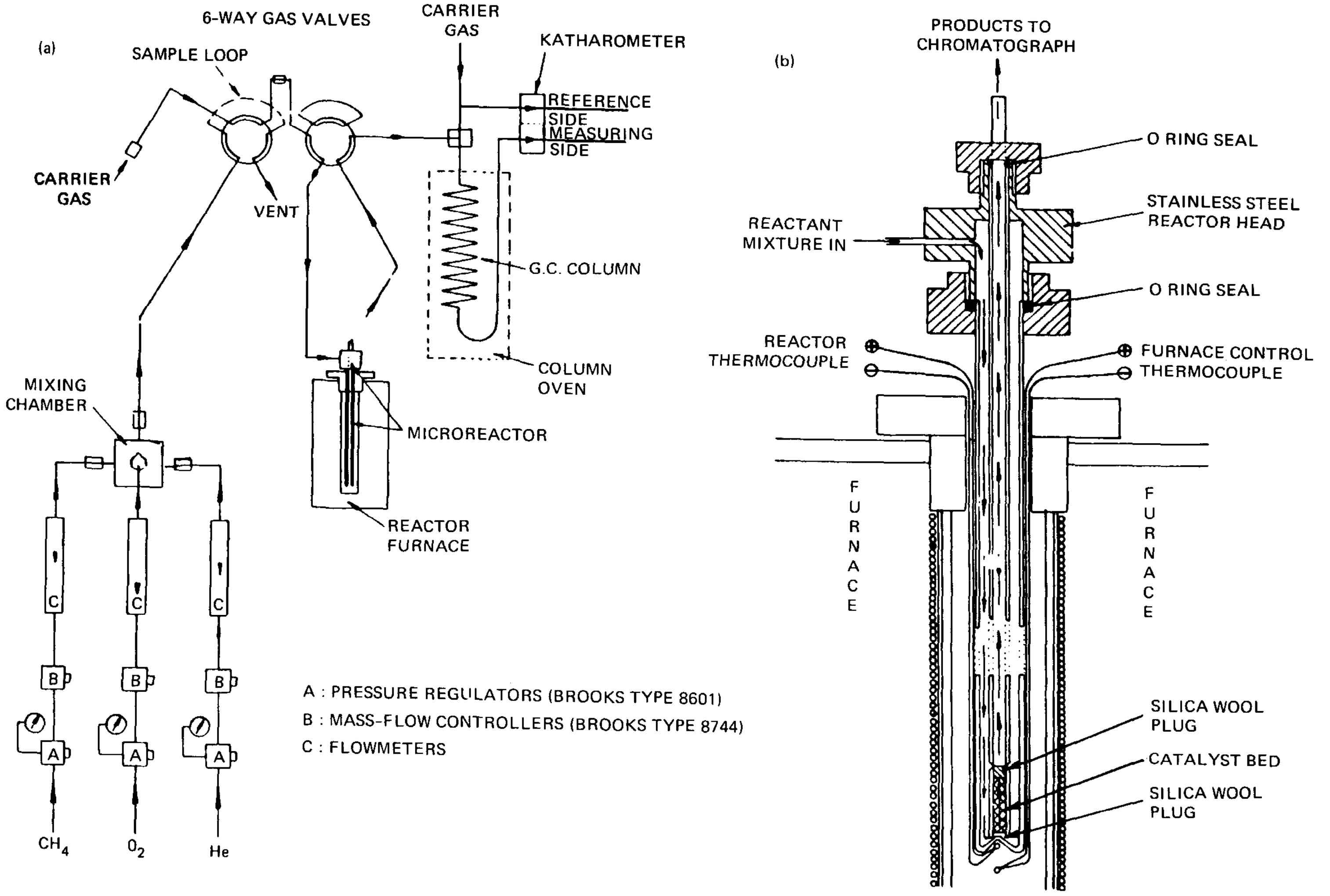

FIG. 1. (a) Pulse-flow microreactor system. (b) The microreactor.

kept in place by silica wool plugs. The flow of the carrier gas, after it had passed through the bed, was carefully monitored in order to detect any resistance to flow caused by a too tightly packed bed. The reactor was placed in an electric furnace, which had a uniform temperature distribution along its length and the temperature of which was electronically controlled. The absence of hot spots, while the reactant gases were passed through the catalyst bed, was checked by means of a thermocouple inserted into the bed.

Precisely monitored reactant gas mixtures were generated using an ultra-high vacuum system, constructed of stainless steel, in which an ultimate vacuum of better than 7×10^{-8} Pa could be obtained. The reactant gases were injected into the carrier gas stream (flow rate, 25 cm^3 min^{-1}) by means of a six-way valve with an associated stainless-steel sample loop, the dimensions of which (30 cm long × 6 mm diam.) were such that a rectangular pulse of the reactants (volume 5 cm^3 at STP unless otherwise stated) underwent minimal mixing with the carrier gas before reaching the catalyst. The sample pulse shape was measured by attaching a microkatharometer (response time 3×10^{-3} s) to the outlet of the six-way valve and the degree of mixing could be found from the concentration profiles of the pulses generated from sample loops of different lengths and diameters. A second six-way valve, connected to the outlet from the first, either diverted the flow through the catalyst or bypassed the microreactor enabling the gases to enter the gas chromatograph directly.

Separation of the reactants and products was carried out by means of a silica gel column (1.8 m long × 6.3 mm diam.) at 323 K, a Carbosieve B column (1.2 m long × 3.2 mm diam.) at 323 K and a Porapak Q column (2.2 m long × 6.3 mm diam.) at 373 K, all with helium as the carrier gas. A katharometer detector, heated to 328 K, was used to analyze oxygen, oxides of carbon and water, and a flame ionization detector, heated to 373 K, was used for the analysis of organic compounds. The presence of formaldehyde was tested colorimetrically by means of its reaction with chromotropic acid.

Characterization of Supported Catalysts

Measurement of surface areas. Dynamic measurements of the surface area of the catalyst supports, involving the adsorption of nitrogen at temperatures close to its boiling point, were carried out using the flow system method developed by Nelsen and Eggertsen (*11*) and improved by Farey and Tucker (*12*). BET surface areas of the samples were calculated from nitrogen adsorption isotherms and agreed well with those found by conventional static methods. The values obtained for titanium(IV) oxide, γ-aluminum(III) oxide, and thorium(IV) oxide were 6.8, 45, and 2.5 m^2 g^{-1}, respectively.

Although the precious metal surface areas were in some cases measured directly by hydrogen adsorption methods, the majority of values were eventually determined from particle size measurements using transmission electron microscopy. Examination of the precious metal particles revealed a spherical symmetry except when the catalyst was exposed to oxygen at high temperatures in which case the particles assumed a hexagonal shape. Hundreds of particles were measured from each catalyst and the metal surface area, S, (in square meters per gram) was obtained from the equation:

$$S = \frac{6 \times 10^4}{\rho d}$$

where ρ is the density of metal (in grams per cubic meter) and d is the diameter of the particles (in meters).

It was found that this method of determining metal surface areas gave values in good agreement with those obtained by chemisorption methods and this has also been shown to be the case by Aben (*13*) and by Paryjczak and Szymura (*14*).

Scanning electron microscopy. Scanning electron micrographs were obtained using a JEOL JSM 35 instrument. In order to prevent charging of the samples, the surface was sputter-coated with a 50-nm-thick layer of gold before examination. The elements present were identified using a dispersive X-ray analyzer; the technique is limited to elements of atomic number greater than 10.

Transmission electron microscopy. The particle size distributions for the precious metals were determined using a JEOL JEM 100C transmission electron microscope. The thin specimens required were prepared by mixing the powdered catalysts with Spurr low-viscosity resin and, after curing, sectioning the product in an ultramicrotome, using a diamond knife. The resulting sections were mounted on a carbon-coated copper grid.

X-Ray photoelectron spectroscopy (XPS). X-Ray photoelectron spectra were obtained using a VG Scientific ESCA Mark II spectrometer. The powdered catalysts were pressed into indium foil prior to being mounted in this instrument and spectra were obtained using aluminum K_α radiation of 1486.6 eV.

RESULTS

Control Experiments

The extent to which homogeneous oxidation of methane occurs at the temperatures concerned was determined by experiments using an empty silica reactor tube. In the range 523–723 K, where most of the heterogeneous oxidation work was carried out, less than 1% of the methane was consumed. Even at 823 K, only ca. 3% of the hydrocarbon reacted.

Similarly the contribution of the various catalyst supports on their own was assessed by exposing them either to methane alone or to a mixture of methane and oxygen (Table 2). Although considerable reaction occurred over tin(IV) oxide, the catalytic effect of all the other supports can be regarded as small, particularly as 873 K is well above the temperature range used in this work for studies of methane oxidation.

TABLE 2

The Effects of some Catalyst Supports on the Thermal Decomposition and Oxidation of Methane at 873 K

Catalyst support	% Conversion of methane	
	CH_4 alone[a]	CH_4 + O_2[b]
TiO_2 (rutile)	1.5	—
TiO_2 (89% anatase + 11% rutile)	1.6	8.6
γ-Al_2O_3	1.1	2.3
ThO_2	0.8	7.1
SnO_2	25	100
SiO_2	1.8	—
Silica reactor tube	—	3.2

[a] Reactant pulse contained 2.8×10^{-7} mol CH_4.

[b] Reactant pulse contained 4.0×10^{-5} mol CH_4 and 1.8×10^{-5} mol O_2.

Measurements were also made of the rate of methane oxidation over some supported catalysts at a temperature of 683 K, all with the same precious metal loading but with the average diameter of the particles of the support varying from 75 to 300 μm. The lack of variation of rate which was observed indicates that interparticle diffusion plays no significant part in the reaction at this temperature.

Oxidation of Methane over Precious Metals

Table 3 compares the activities of a number of supported precious metal catalysts operating under equilibrium conditions. Both the support and the precious metal clearly play a significant part in determining the catalytic activity. An increase in palladium loading on a given support increased the overall rate of methane oxidation for both methane-rich and oxygen-rich mixtures; however, both the activity per unit mass and, to a lesser extent, the activity per unit area of palladium metal decreased with increased loading (Table 3). Similar results were found with platinum for methane-rich mixtures; platinum catalysts supported on γ-Al_2O_3 again exhibited high activity, although in general slightly lower rates of

TABLE 3

The Effects of Catalyst Loading and the Nature of the Support on the Rate of Oxidation of Methane

Supported catalyst	Reaction rate (10^{-2} mol $s^{-1}g^{-1}$ precious metal or (10^{-2} mol $s^{-1}m^{-2}$ precious metal))			
	$CH_4 + 0.45\ O_2$[a]		$CH_4 + 2\ O_2$[b]	
	623 K	683 K	623 K	683 K
2.7 wt% Pd on TiO_2	7.53(1.65)	16.57(3.64)	0.89(0.20)	2.57(0.57)
20 wt% Pd on TiO_2	2.24(0.77)	3.05(1.05)	0.45(0.15)	0.99(0.45)
40 wt% Pd on TiO_2	1.63 (—)	— (—)	0.34 (—)	— (—)
2.7 wt% Pd on γ-Al_2O_3	13.72(3.57)	21.56(5.60)	2.17(0.56)	3.50(0.91)
11 wt% Pd on γ-Al_2O_3	— (—)	6.42(3.34)[c]	0.64(0.34)	1.33(0.69)
2.7 wt% Pd on α-Al_2O_3	5.61 (—)	7.84 (—)	— (—)	— (—)
3.0 wt% Pd on ThO_2	2.21(0.48)	4.99(1.08)	— (—)	— (—)
2.7 wt% Pt on TiO_2	3.77(0.34)	13.60(1.36)	— (—)	— (—)
2.7 wt% Pt on γ-Al_2O_3	11.11(1.11)	18.29(1.84)	— (—)	— (—)
10 wt% Pt on γ-Al_2O_3	5.46 (—)	7.93 (—)[c]	— (—)	— (—)
3.0 wt% Pt on ThO_2	1.36 (—)	4.24 (—)	— (—)	— (—)

[a] Reactant pulse contained 4.0×10^{-5} mol.
[b] Reactant pulse contained 1.8×10^{-5} mol.
[c] All oxygen consumed.

methane oxidation were obtained with platinum than with palladium.

Some studies were made of the effects on catalytic activity of the precursor of the precious metal compound and of the pretreatment of the catalyst. The use of palladium(II) nitrate rather than tetraammine palladium(II) chloride for the preparation of palladium catalysts had no appreciable influence on the subsequent activity. However, mechanical mixing of palladium(II) oxide with titanium(IV) oxide produced a catalyst of significantly lower activity than those obtained by thermal decomposition of palladium(II) nitrate or tetraammine palladium(II) chloride dispersed on the same support. Some examples of the effect of catalyst pretreatment on catalyst activity are shown in Fig. 2. Subsequent exposure to pulses of methane and oxygen of Pd on γ-Al_2O_3 catalysts which had been pretreated in various atmospheres showed that it took some time before equilibration was complete. Catalysts pretreated in a hydrogen + helium mixture were most readily activated but those pretreated with oxygen had a very low activity even after exposure to numerous pulses of methane and oxygen.

Orders of reaction with respect to both methane and oxygen were determined for various supported catalysts at temperatures in the range 580–710 K and using reactant mixtures with $CH_4 : O_2$ ratios varying from 1 : 10 to 10 : 1. With both palladium and platinum catalysts, the order in oxygen tended toward zero, whereas the order in methane was usually about unity. Even at higher temperatures, the orders were found to remain substantially the same.

Rates of methane oxidation (measured in terms of the production of oxides of carbon) were measured as a function of temperature for a number of supported catalysts. Many of the plots of $\log_{10}$ (reaction rate) against reciprocal temperature show a sudden change of slope (Fig. 3), the transition temperature depending on the catalyst, the support, and the composition of the methane–oxygen mixture. Platinum catalysts underwent a sudden increase in activity at this transition temperature. With a 3.0

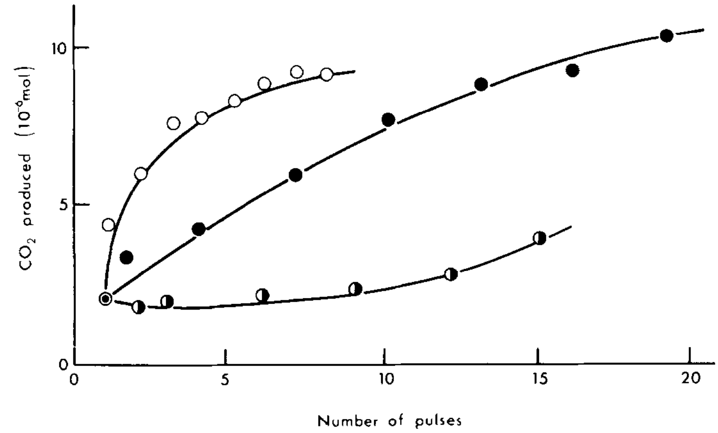

FIG. 2. The effect of catalyst pretreatment on the production of carbon dioxide during methane oxidation over 2.7 wt% Pd on γ-Al_2O_3. Temperature, 683 K; pulse volume, 5 cm^3 (contains 4.2×10^{-5} mol CH_4 and 1.9×10^{-5} mol O_2). (○), Conditioned in H_2 + He at 673 K for 2 h; (●), conditioned in He at 673 K for 2 h; (◑), conditioned in O_2 at 623 K for 1 h and then at 673 K for 1 h.

wt% Pt on ThO_2 catalyst, methane conversion doubled between 642 and 647 K, all oxygen being consumed at the higher temperature. Similarly conversion of methane over a 2.7 wt% Pt on γ-Al_2O_3 catalyst increased by a factor of 8 between 610 and 633 K; carbon monoxide first appeared as a reaction product above 623 K, whereas the quantity of carbon dioxide produced increased only by 10% even up to temperatures as high as 773 K. Palladium catalysts underwent a more gradual transition and

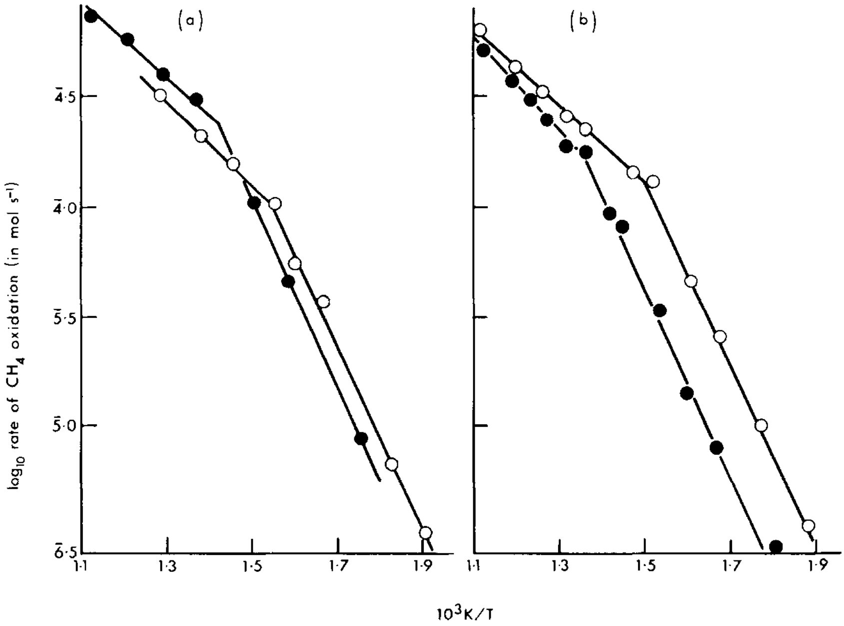

FIG. 3. The variation with temperature of the rate of methane oxidation over some supported catalysts. Pulse volume 5 cm^3 (contains 4.2×10^{-5} mol CH_4 and 1.9×10^{-5} mol O_2). (a) (○), 2.7 wt% Pd on TiO_2; (●), 2.7 wt% Pd on γ-Al_2O_3; (b) (○), 20 wt% Pd on ThO_2; (○), 2.7 wt% Pd on α-Al_2O_3.

here almost all the oxygen was consumed at temperatures well below the transition temperature. Carbon dioxide formation increased continuously with temperature but carbon monoxide began to appear as a product only above the transition temperature.

Values of the activation energy for methane oxidation over a number of supported catalysts are shown in Table 4. Below the transition temperature, the activation energies for platinum catalysts are generally higher than those for palladium catalysts, but above this temperature the reverse is true. The results for palladium in the low temperature region are in good agreement with those obtained by Anderson *et al.* (*1*), viz., 88–92 kJ mol^{-1} for Pd on γ-Al_2O_3, and by Cullis *et al.* (*10*), viz.; 80–90 kJ mol^{-1} for palladium sponge.

In general, an increase in precious metal loading has little effect on activation energies. Changes in reactant composition for a given supported catalyst sometimes alter the transition temperature but generally do not affect the value of the activation energy below this temperature. Finally, studies of the pyrolysis of methane on its own showed that hydrogen was a product at temperatures above 600 K over palladium and that both ethylene and hydrogen were formed at 557 K over platinum.

Adsorption of Oxygen by Supported Precious Metals

Palladium differs from other precious metals in forming a bulk oxide, which is stable between 523 and 1173 K (*15*), within which temperature range the heterogeneous oxidation of methane is almost always studied. Accordingly, the adsorption of oxygen by supported palladium catalysts was measured over a range of temperatures, and comparative measurements were made on a platinum catalyst and on a γ-Al_2O_3 support on its own; in all cases, the catalyst or support was exposed to successive pulses of oxygen until no further adsorption took place. Some values of oxygen uptake are shown in Table 5. The results show, for example, that on a weight basis Pd on γ-Al_2O_3 adsorbs roughly 100 times more oxygen than does a corresponding platinum catalyst. With palladium catalysts, the amount of oxygen adsorbed varies considerably with the nature of the support. Palladium takes up most oxygen when it is supported on γ-Al_2O_3, although alumina on its own does not adsorb appreciable amounts of oxygen and this is found to

TABLE 4

Activation Energies for the Oxidation of Methane over Some Supported Precious Metal Catalysts

Supported catalyst	mol O_2 per mol CH_4	Activation energy (kJ mol^{-1})		Transition point (K)
		Low temp region	High temp region	
2.7 wt% Pd on TiO_2	0.4	83 ± 5	35 ± 3	720
2.7 wt% Pd on γ-Al_2O_3	0.6	84 ± 3	23 ± 3	680
2.7 wt% Pd on α-Al_2O_3	0.4	89 ± 2	45 ± 2	717
11 wt% Pd on γ-Al_2O_3	2	84 ± 5	[a]	—
2.7 wt% Pd on γ-Al_2O_3 + SiO_2	0.4	92 ± 4	45 ± 2	683
2.7 wt% Pd on ThO_2	0.4	85 ± 5	34 ± 3	654
2.7 wt% Pd on ThO_2	2	95 ± 6	24 ± 2	707
20 wt% Pd on SnO_2[b]	2	75 ± 7	[a]	—
2.7 wt% Pt on TiO_2	0.4	116 ± 4	19 ± 2	610
2.7 wt% Pt on γ-Al_2O_3	0.4	114 ± 4	24 ± 2	630
3.1 wt% Pt on ThO_2	0.4	108 ± 3	22 ± 2	644

[a] No change to lower activation energy.

[b] Significant contribution from the support possible in this case (see Table 2).

TABLE 5

Uptake of Oxygen by Some Supported Catalysts[a]

	Oxygen uptake			
	10^{-3} mol O_2 per g of precious metal		10^{-3} mol O_2 per m^2 of precious metal	
	623 K	683 K	623 K	683 K
2.7 wt% Pd on TiO_2	0.9	—	—	—
8.7 wt% Pd on TiO_2	0.2	0.3	0.004	0.006
1.0 wt% Pd on γ-Al_2O_3	5.0	9.0	—	—
2.7 wt% Pd on γ-Al_2O_3	4.2	7.3	—	—
11 wt% Pd on γ-Al_2O_3	1.5	2.7	0.081	0.146
25 wt% Pd on γ-Al_2O_3	1.3	2.5	0.070	0.135
5.0 wt% Pd on ThO_2	0.2	0.2	—	—
5.0 wt% Pt on γ-Al_2O_3	0.02	0.02	—	—
(γ-Al_2O_3)	(0.005)[b]	(0.005)[b]	—	—

[a] Catalyst volume, 0.05 cm^3; pulse volume, 0.25 cm^3.
[b] Oxygen uptake per g of support.

be the case even at temperatures as high at 923 K. However, after γ-Al_2O_3 had been conditioned in flowing helium at 783 K for 3 h, it adsorbed 10 times more oxygen than it did before, presumably because the helium had reversibly removed any loosely bound oxygen present. With Pd on γ-Al_2O_3 and Pd on TiO_2 catalysts, the oxygen uptake at equilibrium per unit mass of precious metal (and the rate of oxygen adsorption) decreased with increasing palladium loading.

Examination of the uptake of oxygen per unit surface area of precious metal indicates that the amount adsorbed by Pd on γ-Al_2O_3 is even greater than for Pd on TiO_2 on a weight basis. Figure 4 shows that the optimum temperature for adsorption of oxygen on a Pd on γ-Al_2O_3 catalyst is 873 K and that thereafter the amount of oxygen taken up falls off rapidly with increasing temperature until at 923 K adsorption is negligible. In contrast, palladium supported on TiO_2 or ThO_2 adsorbed less oxygen but the oxides once formed appeared to be more stable.

Studies of the variation with temperature of the rate of oxygen uptake on various supported catalysts gave activation energies for the adsorption of oxygen ranging from 22.8 to 61.0 kJ mol^{-1}. Comparison of these values with those obtained for the oxidation of bulk palladium metal, viz., 71.4 kJ mol^{-1} (*15*) and 84.0 kJ mol^{-1} (*16*) suggests that, when low loadings of palladium were used, significantly lower activation energies for oxygen adsorption were obtained, whereas higher loadings gave higher values approaching those for oxidation of the bulk metal.

Further experiments showed that there was a good correlation between the amounts of oxygen adsorbed by a sup-

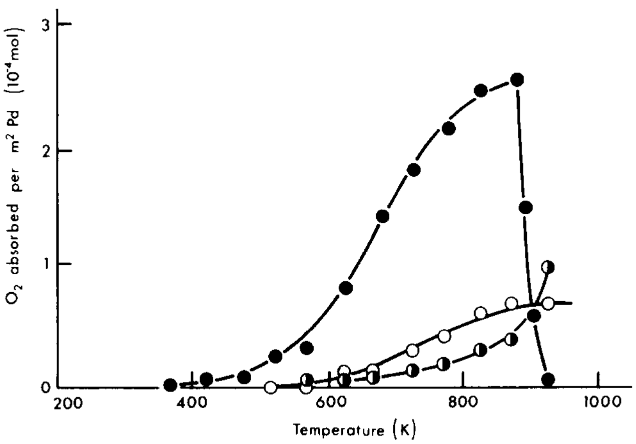

FIG. 4. The variation with temperature of the adsorption of oxygen on supported palladium catalysts. (○), 8.7 wt% Pd on TiO_2 (O_2 pulse volume, 0.25 cm^3); (●), 11 wt% Pd on γ-Al_2O_3 (O_2 pulse volume, 0.50 cm^3); (◑), 5.0 wt% Pd on ThO_2 (O_2 pulse volume, 0.25 cm^3).

ported palladium catalyst at various temperatures and the extents of methane oxidation (as measured by the amounts of carbon dioxide produced) over the same temperature range (Fig. 5). The importance of oxygen adsorbed on the catalyst in the oxidation of methane was confirmed by studies of Pd on TiO_2 catalysts which had previously been reduced at 550 K with 1-cm^3 pulses of hydrogen before being exposed to methane–oxygen mixtures at temperatures increasing from 573 K by steps of 20 K. The two catalysts examined (5.0 wt% Pd on ThO_2 and 2.7 wt% Pd on TiO_2) both showed an abnormally low activity with the first pulse until a certain temperature was reached (633 K for the ThO_2-supported catalyst and 653 K for the TiO_2-supported catalyst), above which identical activity was observed for the first and all subsequent pulses. This suggests that there is competition for oxygen between palladium to form the oxide and methane to undergo oxidation. At low temperatures the first reactant pulse is not in equilibrium with the surface during the oxidation of methane but the use of higher temperatures presumably favors palladium oxidation at the expense of methane oxidation. Preoxidation of the catalyst before exposure to pulses of methane and oxygen had little effect on methane conversion for all pulses between 650 and 700 K. However, from 725 to 775 K the first reactant pulse gave a lower methane conversion than subsequent pulses. Thus an oxygen-rich surface at these temperatures inhibited methane oxidation in the first pulse, equilibrium being achieved only on passage of a second pulse through the catalyst.

Oxidation of Methane by Palladium(II) Oxide and Platinum(IV) Oxide

Pulses of oxygen were first passed over palladium(II) and platinum(IV) oxides, in both unsupported and supported form, at various temperatures; a pulse of methane was then passed over the oxidized catalyst and the carbon dioxide produced was measured. Platinum(IV) oxide was the more active oxidant (Fig. 6), requiring lower temperatures for methane oxidation and for the production of carbon monoxide. The variation of the rate of reaction with initial methane concentration gave orders in methane of 0.8 and 0.6 for palladium(II) and platinum(IV) oxides, respectively. Mea-

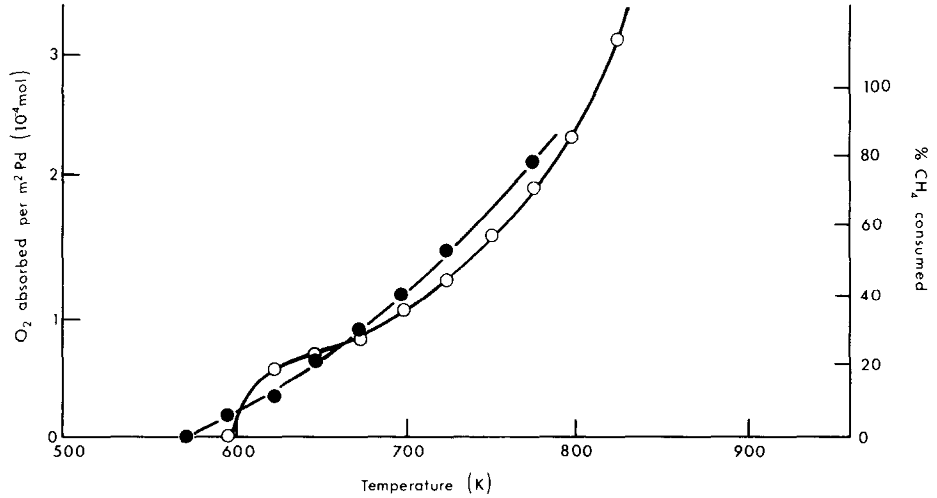

FIG. 5. The variation with temperature of the adsorption of oxygen by and the catalytic activity of a 2.7 wt% Pd on TiO_2 catalyst. (○), Oxygen adsorption (O_2 pulse volume, 0.25 cm^3): (●), methane conversion (pulse volume, 5 cm^3 (contains 2.2×10^{-6} mol CH_4 and 5.9×10^{-6} mol O_2)).

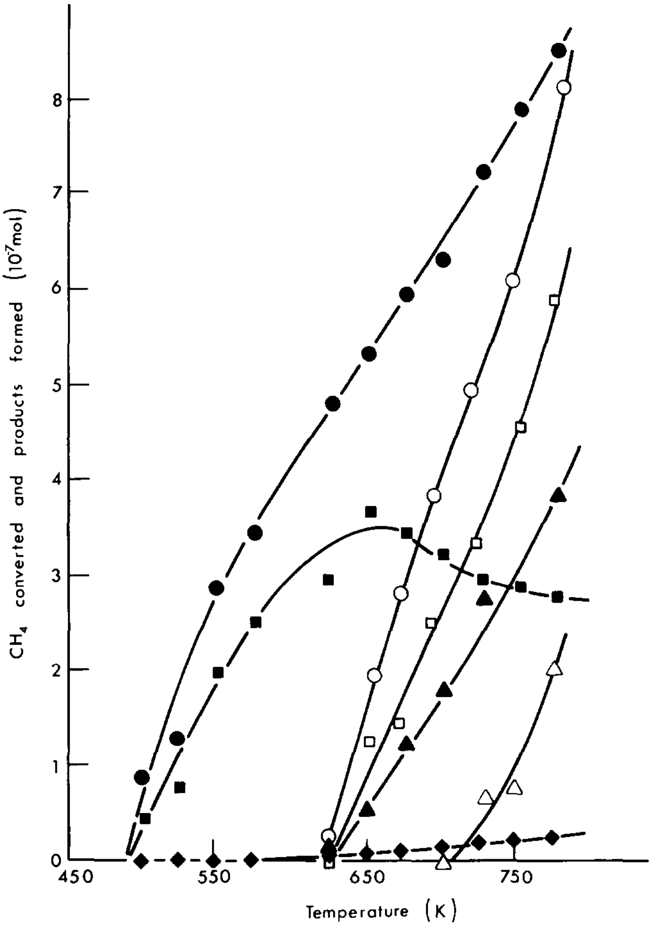

FIG. 6. The oxidation of methane by adsorbed oxygen. Pulse volume, 0.5 cm^3 (contains 1.04 × 10^{-6} mol CH_4). Open symbols: 2.7 wt% PdO on ThO_2. (○), CH_4 converted; (□), CO_2 produced; (△), CO produced. Closed symbols: 2.7 wt% PtO_2 on ThO_2. (●), CH_4 converted; (■), CO_2 produced; (▲), CO produced; (◆), O_2 produced.

surements of the rate of methane oxidation by both the unsupported precious metal oxides gave the activation energies shown in Table 6.

The amount of oxygen adsorbed by the catalyst was, on a molar basis, at least twice that of the methane in a reactant pulse, ensuring that there was enough oxygen to oxidize all the methane present to carbon dioxide and water. The difference between the amounts of methane consumed and of carbon dioxide produced indicated, however, that not all the methane which reacted was completely oxidized. No formaldehyde could be detected among the

TABLE 6

Activation Energies for the Reaction of Methane over Previously Oxidized Palladium and Platinum Catalysts

Catalyst	Temperature range (K)	Activation energy (kJ mol^{-1})
PdO[a]	500–600	48 ± 2
2.7 wt% Pd on ThO_2[b]	625–750	39 ± 3
2.7 wt% Pd on ThO_2[c]	640–755	51 ± 4
PtO_2[a]	500–600	55 ± 3
2.7 wt% Pt on ThO_2[c]	550–773	23 ± 2

[a] Oxidized at 675 K.
[b] Oxidized at 775 K.
[c] Oxidized at 625 K.

products but at least some of the methane was pyrolyzed to carbon that was not recoverable.

There were significant differences in the catalytic activity of palladium(II) oxide depending on the oxidation procedure used. Oxidation under relatively mild conditions (pulses of 0.1 cm^3 of oxygen passed through the catalyst at 625 K) caused no subsequent loss in activity. However, more vigorous oxidation (oxygen flowing continuously through the catalyst for 20 min at 775 K) caused a sharp loss in activity, which reduction with hydrogen followed by reoxidation failed to restore. In contrast, platinum(IV) oxide, when exposed to vigorous oxidation, suffered no decrease in catalytic activity. In accordance with this, scanning electron microscopy showed that "fresh" palladium(II) oxide consisted of particles, ca. 250 μm in diameter, which on exposure to oxygen at 775 K agglomerated, forming loosely bound clumps, ca. 2 mm. in diameter, whereas platinum(IV) oxide underwent no change in morphology as a result of the same treatment. However, during oxidation of PtO_2, a platinum mirror formed on the walls of the reactor tube and this indicates the greater volatility of platinum(IV) oxide compared with that of palladium(II) oxide. This behavior was observed for both unsupported and supported catalysts and may well impose a limit on the useful lifetime of platinum catalysts under these conditions.

The Size of the Precious Metal Particles in Supported Catalysts

A number of supported catalysts were examined by transmission electron microscopy and measurements were made of the average size of the precious metal particles, which were identified as black spots against the lighter background of the support. Particle sizes could not be determined for palladium and platinum on thorium(IV) oxide or for palladium on tin(IV) oxide, because the precious metals were indistinguishable from the support. In addition, with low loadings (e.g., 2.7 wt%) of palladium (formed from tetraammine palladium(II) chloride) on titanium(IV) oxide, the palladium was not visible under the electron microscope.

For a given support, the size of the precious metal particles increases with metal loading, although it depends also on the method of preparation of the metal (Table 7). Thus increased loading does not necessarily lead to improved dispersion of the metal but rather to agglomeration of the particles. The effect of prolonged heating on the size of the palladium particles in a 2.7 wt% Pd on γ-Al_2O_3 catalyst is shown in Fig. 7. The catalyst was treated in flowing air at 823 K for 40 days and its activity toward methane oxidation was measured periodically. In addition, the size distribution

TABLE 7

Sizes of Precious Metal Particles in Supported Catalysts[a]

Supported catalyst[b]	Mean diameter of metal particles (nm)	Range of diameter of metal particles (nm)
2.7 wt% Pd on TiO_2[c]	11	2–32
8.5 wt% Pd on TiO_2[c]	13	2–26
8.7 wt% Pd on TiO_2[d]	10	2–26
2.7 wt% Pd on γ-Al_2O_3	13	2–32
11 wt% Pd on γ-Al_2O_3	26	<1–70
25 wt% Pd on γ-Al_2O_3	26	5–70
2.7 wt% Pd + Pt (3 : 1) on TiO_2[e]	4.0	<1–20
2.7 wt% Pt on TiO_2[f]	2.4	<1–14
2.7 wt% Pt on γ-Al_2O_3	2.8	<1–9

[a] Accelerating voltage, 100 kV; magnification, ×50,000 to ×300,000.

[b] All catalysts were conditioned in flowing helium (25 cm^3 min^{-1}) at 773 K for 16 h before being exposed to methane–oxygen pulses at 773 K; 11 wt% Pd on γ-Al_2O_3 catalyst was subsequently heated to 923 K in the presence of oxygen.

[c] Prepared from palladium(II) oxide.

[d] Prepared from tetraammine palladium(II) chloride.

[e] Prepared from tetraammine platinum(II) chloride and tetraammine palladium(II) chloride.

[f] Prepared from tetraammine platinum(II) chloride.

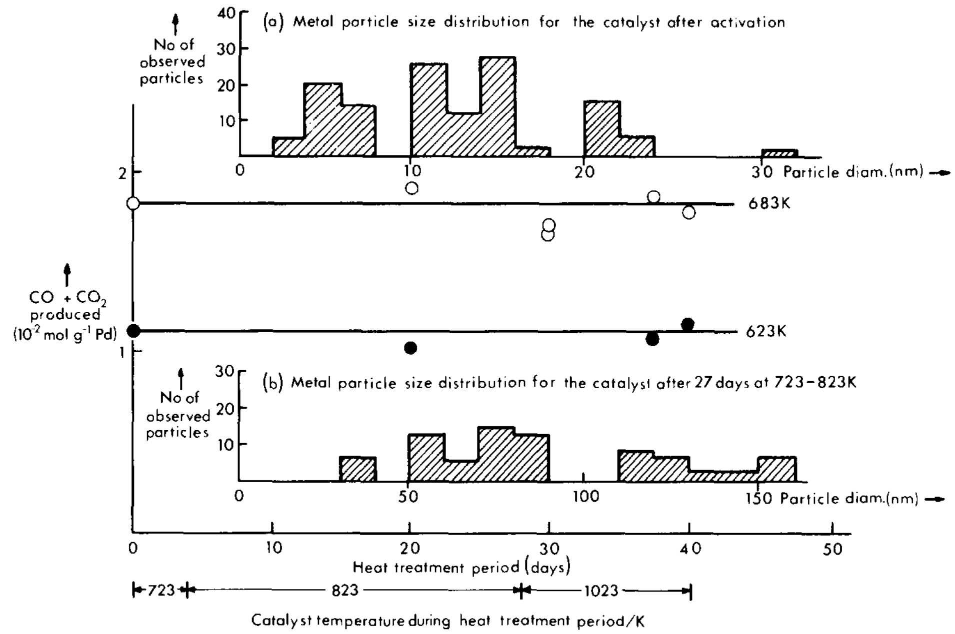

FIG. 7. The effect of prolonged heating in air on the catalytic activity and metal particle distribution of a 2.7 wt% Pd on γ-Al_2O_3 catalyst.

of the palladium particles was measured both before and after heat treatment. It can be seen that, while the production of oxides of carbon and hence the activity per gram of palladium is almost unaffected by heating, the particle size increases considerably.

Evidence that the smaller particles encourage the formation of palladium(II) oxide in supported palladium catalysts was obtained by means of X-ray photoelectron spectroscopy. Examination of the $Pd_{3d_{3/2}}$ and $Pd_{3d_{5/2}}$ binding energies showed that a high loading of palladium on titanium(IV) oxide (40 wt% Pd on TiO_2) exhibited metallic character, while a catalyst with a low metal loading (2.7 wt% Pd on TiO_2) contained palladium(II) oxide (Table 8). Exposure of a 2.7 wt% Pd on γ-Al_2O_3 catalyst to a methane-rich mixture left the palladium in a state intermediate between that of the metal and the oxide.

DISCUSSION

General Considerations

The kinetics of methane oxidation over supported precious metal catalysts were studied in a region in which the rate of reaction was controlled only by the chemical processes occurring on the catalyst surface. Homogeneous oxidation of methane was insignificant over the temperature range

TABLE 8

Electron Binding Energies for Palladium Metal, Palladium Compounds and Supported Palladium Catalysts

Material	Binding energies (eV)	
	$Pd_{3d_{5/2}}$	$Pd_{3d_{3/2}}$
Pd	335.1	340.5
PdO	338.2	343.6
$Pd(NH_3)_4Cl_2$	337.0	343.3
2.7 wt% Pd on TiO_2[a]	338.5	343.9
40 wt% Pd on TiO_2[a]	336.1	341.1
5.1 wt% PdO on TiO_2[a]	338.6	344.1
18.7 wt% PdO on TiO_2[a]	338.7	344.2
2.7 wt% Pd on γ-Al_2O_3[a]	336.4	—

[a] Conditioned at 773 K for 16 h in flowing helium and then exposed to pulses of methane-rich mixtures at 673 K.

where the heterogeneous reaction was investigated. Interparticle diffusion was also shown to be absent at the temperatures at which the kinetics were studied for at least some supported catalysts and chromatographic effects of the reactant pulse were avoided by the use of a sufficiently large pulse (5 cm^3).

The supports themselves, with the exception of tin(IV) oxide, did not appreciably catalyze either the pyrolysis or the oxidation of methane below 723 K (Table 2). However, the nature of the support did have some significant effects on the catalytic activity of the precious metals (Table 3).

The Adsorption of the Reactants

The adsorption of oxygen on the catalyst surface is an essential step in the oxidation of methane over precious metal catalysts and indeed a good correlation was found between oxygen uptake and methane conversion. Optimum activity for methane oxidation was achieved only when sufficient oxygen was adsorbed from the gaseous reactant mixture onto a previously reduced palladium surface. Examination by XPS of a supported palladium catalyst which had been exposed to pulses of methane and oxygen showed that the palladium had similar binding energies to those obtained for palladium(II) oxide (Table 8). Indeed, the presence of this oxide was still observed when the reactant mixture contained less than stoicheiometric amounts of oxygen. Even under reducing conditions, therefore, not all the adsorbed oxygen was consumed. On the other hand, a surface that was exposed to oxygen at temperatures above 725 K did not favor methane oxidation. Thus equilibrium between the catalyst and the gaseous reactants was achieved only when the palladium surface was partially covered with oxygen. This is in agreement with observations of adsorption of oxygen prior to oxidation of C_1–C_4 alkanes over catalytic beads (*9*).

The zero-order dependence of the rate on oxygen concentration, observed with palladium and platinum catalysts, suggests that oxygen is strongly bound to the surface. The formation of a layer of oxygen on the surface of these metals is accompanied at high temperatures by migration of oxygen into the bulk of the palladium (*15*). Conrad *et al.* (*17*) revealed that oxygen may exist in two different states on a Pd(111) surface as well as below the surface. At low temperatures, reactive chemisorbed oxygen is present which is desorbed at around 900 K. Treatment of palladium with oxygen at 1000 K, however, provides a tightly bound surface species which is chemically stable and may well represent an intermediate stage in the formation of palladium(II) oxide. This nonreactive oxygen would explain the lack of activity observed when palladium is exposed to oxygen at temperatures above 725 K.

This behavior of palladium is mirrored by platinum as Pt(111) (*18*). Below 800 K, chemisorbed oxygen is present which reacts with hydrogen and carbon monoxide even at room temperature and the oxide of the precious metal decomposes completely above 1000 K. When a Pt(111) surface is exposed to oxygen at or above 800 K, an oxide is formed which is unreactive towards hydrogen and carbon monoxide and which decomposes only slowly at 1200 K. However, in the case of platinum, although the high temperature oxide appears to be formed below the surface of the metal (*18*), substantial uptake of oxygen into the bulk of the metal does not occur.

In addition to geometric factors, there are differences in the electronic structures of palladium–oxygen bonds. In the case of a Pd(111) surface, oxygen may bond with either the *sp* orbitals of the precious metal or with the *d* orbital. The *sp*–2*p* (Pd–O) bonding appears to involve oxygen which is below the surface of the metal. This *sp* bonding with the oxygen 2*p* orbital has also been observed for nickel–oxygen bonding (*19*). On platinum, however, only the *d* orbitals are involved with strong attenuation of the orbital peak during oxygen adsorption.

At the temperatures used in the present work (673–873 K), it is probably migration of oxygen into the bulk as well as surface adsorption that is being studied. The oxygen uptake depended both on the support and on the dispersion of the precious metal on it (Table 5). As the metal : support ratio increased, the oxygen uptake fell off, due presumably to the inability of the larger palladium particles, obtained under conditions where the metal was not well dispersed, to adsorb sufficient oxygen. Indeed, XPS showed that there was more metallic character in supported palladium at higher loadings.

The extent to which the catalyst adsorbed oxygen was not dependent on particle size alone. There are considerable variations in the stoicheiometry of oxygen chemisorption on precious metals, especially when these are dispersed on supports (*20, 21*). Maire *et al.* (*22*) found, using Auger electron spectroscopy, that different crystal planes of platinum have different reactivities toward oxygen. For a Pt(100) surface, oxygen adsorption occurs at lower temperatures than on Pt(111). In addition, in the case of Pd(111), oxygen was found by Weissman *et al.* (*19*) to be adsorbed on sites on the terraces, whereas on Pt(111) oxygen is adsorbed almost exclusively on sites at steps and defects. For a supported catalyst which is almost certainly polycrystalline, the situation will be more complex with many crystal planes of different reactivities present. It seems likely that the support will have an effect on the crystallinity of the precious metal and this will determine the ability of the metal to adsorb oxygen. For a polycrystalline foil, Maire *et al.* (*22*) found that the amount of oxygen adsorbed per surface platinum atom lay between the highest and lowest values obtained for oxygen adsorption on six different crystal planes.

Adsorption of methane at temperatures similar to those required for its oxidation is probably dissociative, since hydrogen was formed during pyrolysis of methane over both palladium and platinum. In addition, some of the carbon left on the catalyst surface could be reconverted to methane when hydrogen was passed through the catalyst bed. If the palladium surface is covered with oxygen, methane may possibly be adsorbed on a layer of oxygen. There is little information concerning the adsorption of hydrocarbons on palladium(II) oxide, as oxidation normally accompanies adsorption. It has been postulated that both methane and oxygen can be adsorbed on an isolated single palladium atom on a zeolite support (*4*).

An explanation for the differences observed between palladium and platinum in their behavior toward the oxidation of methane may perhaps be found in the different abilities of these metals to adsorb the reactant gases. Palladium, unlike platinum, can absorb oxygen into its bulk, thus providing a reservoir of oxygen which may prevent methane pyrolysis on its surface. In addition, a greater proportion of the surface of platinum is available for the adsorption and subsequent pyrolysis of methane. Cullis *et al.* (*10*) found that only 20% of the active surface of a palladium catalyst was covered by carbonaceous products following methane pyrolysis at 753 K, while Trimm and Lam (*8*) observed over 40% coverage by carbon of a supported platinum catalyst at 773 K. In the present work, no loss in activity for methane oxidation was observed on passage of successive methane-rich pulses through a palladium catalyst, although methane alone caused sooting of the surface, resulting in complete deactivation after 20 pulses.

Kinetics of Methane Oxidation

The experimental finding that the rate of methane oxidation is proportional to the first power of the methane concentration but independent of the oxygen concentration suggests a mechanism involving the reaction of methane with strongly adsorbed oxygen. A similar conclusion was reached by Mezaki and Watson (*3*) and Cullis and Nevell (*9*).

Most of the Arrhenius plots exhibit a well-defined discontinuity (Fig. 3). Apparent activation energies for palladium catalysts at temperatures below the transition point are in good agreement with previously reported values (*1, 10*). As oxygen is strongly adsorbed on the precious metal, the true activation energy for the surface reaction is given by:

$$E_{\mathrm{A\,true}} = E_{\mathrm{A\,apparent}} - \tfrac{1}{2}\Delta H_{\mathrm{O_2ads}}$$

where $\Delta H_{\mathrm{O_2ads}}$ is the heat of adsorption of oxygen on the precious metal surface. Unfortunately, the heat of adsorption of oxygen on both platinum and palladium decreases with coverage. Nevertheless, initial heats of chemisorption of oxygen on palladium and platinum were found to be 286 and 269 kJ mol^{-1}, respectively (*23*). Zakumbaeva and Artamonov (*24*) observed a value of 286 kJ mol^{-1} falling to 88 kJ mol^{-1} at a temperature of 310 K for 4 wt% Pd on Al_2O_3, the rate of decrease of the heat of adsorption becoming greater at higher coverages. As the surface coverage of platinum by oxygen is lower than that of palladium, the heat of adsorption of oxygen on palladium may well fall below that of platinum. In such a case, the heat of adsorption of oxygen may be related to the catalytic activity of the metal oxide for methane oxidation, because, as has been seen, it is a chemisorbed oxygen species that is reactive. This is in agreement with the results of Moro-oka *et al.* (*25*), who related the heat of formation of the catalyst oxide to the activity of the catalyst.

There appears to be a relationship between the apparent activation energies observed for the oxidation of methane in the presence and in the absence of oxygen. With a PdO on ThO_2 catalyst, the activation energy for methane oxidation was 39 kJ mol^{-1} and the corresponding value for oxidation of a 5 wt% Pd on ThO_2 catalyst was 47 kJ mol^{-1}. The sum of these two values is 86 kJ mol^{-1}, which agrees well with the activation energy for methane oxidation below the transition point (85 kJ mol^{-1}) (Table 9). The overall activation energy at lower temperatures may thus perhaps be expressed as the sum of the activation energies for oxidation of palladium and for methane oxidation by the resulting palladium oxide. On the other hand, the activation energy for methane oxidation over 2.7 wt% PtO_2 on ThO_2 corresponds to that obtained above the transition point. This suggests that, under these conditions, oxida-

TABLE 9

Energies of Activation for the Oxidation of Methane in the Presence and Absence of Gaseous Oxygen over Supported Precious Metal Catalysts and for the Oxidation of These Catalysts

Supported catalyst	Activation energy for methane oxidation in the presence of gaseous oxygen		Activation energy for methane oxidation in the absence of gaseous oxygen (kJ mol^{-1})	Activation energy for the oxidation of the precious metal (kJ mol^{-1})
	Below the transition point (kJ mol^{-1})	Above the transition point (kJ mol^{-1})		
2.7 wt% Pd on TiO_2	83	35	23	43
2.7 wt% Pd on γ-Al_2O_3	89	45	—	45
2.7 wt% Pd on ThO_2	85	34	39	47
3.1 wt% Pt on ThO_2	108	22	23	—

tion of the precious metal is no longer an important step in the reaction mechanism.

The sudden changes in activation energy observed (Fig. 3) may be connected with a transition from chemical control to diffusion limitation. As the essentially nonporous thorium(IV) oxide underwent transition at lower temperatures than the porous γ-Al_2O_3, mass transfer limitations may be interparticle or bulk rather than intraparticle. Furthermore, in the case of platinum catalysts, the apparent activation energies above the transition point were considerably less than half those below it, whereas for pore diffusion, the activation energy is reduced to one half (*26*). Kinetic measurements of the oxidation of methane were carried out at temperatures well below this transition point and in the temperature range in which the absence of interparticle diffusion was confirmed for 2.7 wt% Pd on TiO_2. Measurements taken in this region thus represent true chemical control; above these temperatures diffusion limitation in pores, possibly coupled with mass transfer control of reactants to the surface, will determine the rate of reaction.

There was a rapid rise in the catalytic activity of supported platinum catalysts at the transition point over a temperature range of less than 1 K. Similar behavior was observed by Schwartz *et al.* (*27*) during oxidation of hydrocarbons over a platinum wire and this was attributed to a transition from a region of kinetic control to one of diffusion control. This rapid rise in activity may be explained in terms of thermal as well as mass transfer effects. Weisz and Hicks (*28*) demonstrated that, for a catalyst pellet undergoing localized overheating, the rate of reaction will depend on the temperature gradient set up throughout the pellet. In the case of the supported platinum catalysts used in the present work, the pore sizes of the supports are large compared with the mean free path of the reactants and the thermal conductivities of the supports lie in the range 4–13 $W\ m^{-1}\ K^{-1}$ (*29*). These properties would encourage thermal inhomogeneities. However, the largest increase in reaction rate was observed for platinum supported on γ-Al_2O_3, which would not be predicted from the relative thermal conductivities of the supports (γ-Al_2O_3, 12.97 $W\ m^{-1}\ K^{-1}$; TiO_2, 3.92 $W\ m^{-1}\ K^{-1}$; ThO_2, 5.86 $W\ m^{-1}\ K^{-1}$; all at 673 K).

Some explanation for the behavior of platinum on γ-Al_2O_3 may be found from consideration of the porosity of the support. Trimm and Lam (*8*) noticed a sudden rise in activity for the oxidation of methane over platinum supported on porous SiO_2/Al_2O_3 fibers under methane-rich conditions. This sharp increase was believed to be due to cracking of methane on the catalyst, the subsequent oxidation of the hydrogen so produced causing a sudden rise in temperature and hence in methane conversion. The fact that this occurred for a porous but not a nonporous catalyst support was tentatively ascribed to the localization and subsequent oxidation of the products of cracking in the pores.

Influence of Precious Metal Particle Size

A comparison of the particle sizes of palladium supported on titanium(IV) oxide and on aluminum(III) oxide, measured by transmission electron microscopy, revealed improved dispersions of the precious metal over the former support (Table 8). Adsorption of oxygen, however, was significantly greater on 2.7 wt% Pd on γ-Al_2O_3 than on 2.7 wt% Pd on TiO_2 (Table 5).

Increases in metal particle size are dependent on the temperature, the time for which the catalyst is kept at that temperature, the metal loading, and the nature of the support and of the surrounding atmosphere. Platinum on γ-alumina catalysts are normally more resistant to sintering in nitrogen or hydrogen than the corresponding palladium catalysts, while the opposite is true in oxygen or air (*30, 31*). Although the average diameter of the metal particles in a 2.7 wt% Pd on γ-Al_2O_3 catalyst increased from 14 to 80 nm, the catalytic activity toward methane oxidation changed little (Fig.

7). This means that the rate of methane oxidation is independent of metal particle size under methane-rich conditions. In this connection, Carballo and Wolf (*32*) found that alterations in the average particle diameters of palladium supported on γ-alumina had little effect on the rate of propene oxidation.

Prolonged heating may affect also the surface area of the support as a result of structural and phase changes. Nevertheless, massive agglomeration of the precious metal would be expected before these changes become significant.

ACKNOWLEDGMENT

The authors thank J. and S. Sieger Limited for valuable support of this work.

REFERENCES

1. Anderson, R. B., Stein, K. C., Feenan, J. J., and Hofer, L. J. E., *Ind. Eng. Chem.* **53,** 809 (1961).
2. Schwab, G. M., and Watson, A. M., *J. Catal.* **4,** 570 (1965).
3. Mezaki, R., and Watson, C. C., *Ind. Eng. Chem. Process Des. Dev.* **5,** 62 (1966).
4. Firth, J. G., and Holland, H. B., *Nature (London)* **217,** 1252 (1968).
5. Firth, J. G., and Holland, H. B., *Trans. Faraday Soc.* **65,** 1121 (1969).
6. Cullis, C. F., Nevell, T. G., and Trimm, D. L., *J. Chem. Soc. Faraday Trans. 1* **68,** 1406 (1972).
7. Zozulya, A. D., *Nauchn. Soobshch. Inst. Gorn. Dela A. A. Skochinskogo* **142,** 68 (1976).
8. Trimm, D. L., and Lam, C. W., *Chem. Eng. Sci.* **35,** 1405 (1980).
9. Cullis, C. F., and Nevell, T. G., *Proc. R. Soc. Ser. A* **349,** 523 (1976).
10. Cullis, C. F., Keene, D. E., and Trimm, D. L., *Trans. Faraday Soc.* **67,** 864 (1971).
11. Nelsen, F. M., and Eggertsen, F. T., *Anal. Chem.* **30,** 1387 (1958).
12. Farey, M. G., and Tucker, B. G., *Anal. Chem.* **43,** 1307 (1971).
13. Aben, P. C., *J. Catal.* **10,** 224 (1968).
14. Paryjczak, T., and Szymura, J. A., *Z. Anorg. Allg. Chem.* **449,** 105 (1979).
15. Campbell, C. T., Foyt, D. C., and White, J. M., *J. Phys. Chem.* **81,** 491 (1977).
16. Ertl, G., and Koch, J., *in* Adsorption–Desorption Phenomena (F. Ricca, Ed.), p. 345. Academic Press, New York, 1973.
17. Conrad, H., Ertl, G., Küppers, J., and Latta, E. E., *Surf. Sci.* **65,** 245 (1977).
18. Niehus, M., and Comsa, G., *Surf. Sci. Lett.* **93,** L147 (1980).
19. Weissman, D. L., Shek, M. L., and Spicer, W. E., *Surf. Sci. Lett.* **92,** L59 (1980).
20. Sermon, P. A., *J. Catal.* **24,** 467 (1972).
21. Wilson, G. R., and Hall, W. K., *J. Catal.* **24,** 306 (1972).
22. Maire, G., Légaré, P., and Lindauer, G., *Surf. Sci.* **80,** 238 (1979).
23. Brennan, D., Hayward, D. O., and Trapnell, B. M. W., *Proc. R. Soc. Ser. A* **256,** 81 (1960).
24. Zakumbaeva, G. D., and Artamonov, S. V., *React. Kinet. Catal. Lett.* **10,** 183 (1979).
25. Moro-oka, Y., Morikawa, Y., and Ozaki, A., *J. Catal.* **7,** 23 (1967).
26. Satterfield, C. N., and Sherwood, T. K., The Role of Diffusion in Catalysis. Addison–Wesley, Reading, Mass., 1963.
27. Schwartz, A., Holbrook, L. L., and Wise, H., *J. Catal.* **21,** 199 (1971).
28. Weisz, P. B., and Hicks, J. S., *Chem. Eng. Sci.* **17,** 265 (1962).
29. Powell, R. W., Ho, C. Y., and Lilley, P. E., Thermal Conductivity of Selected Materials. National Standard Reference Data Ser, No. 8. National Bureau of Standards, Washington, D.C., 1966.
30. Swift, H. E., Lutinski, F. E., and Tobin, H. H., *J. Catal.* **5,** 285 (1966).
31. Dodgson, I. L., and Webster, D. E., *in* Preparation of Catalysts (B. Delmon, P. A. Jacobs, and G. Poncelet, Eds.), p. 279. Elsevier, Amsterdam, 1976.
32. Carballo, L. M., and Wolf, E. E., *J. Catal.* **53,** 366 (1978).